Design and Characterization of a Low-Temperature Plasma Reactor for Seed Treatment Applications

A Study on Ozone and Reactive Species Generation

Bram van de Ruit & Teun Mertens

Delft University of Technology

TU Delft

Design and Characterization of a Low-Temperature Plasma Reactor for Seed Treatment Applications

A Study on Ozone and Reactive Species Generation

by

Bram van de Ruit & Teun Mertens

Instructors: dr.ing. H.W. van Zeijl, Em. Prof.dr.ir. J. van Turnhout, drs. L. Wymenga
Project Duration: April, 2025 - June, 2025
Faculty: Faculty of Electrical Engineering, Delft

Cover: Bram van de Ruit & Teun Mertens
Style: TU Delft Report Style, with modifications by Daan Zwaneveld

TU Delft

Abstract

This thesis presents the design and characterization of a low-temperature plasma reactor for seed treatment applications, with a focus on the generation of ozone. The research will look at two different setups using dielectric barrier discharge (DBD) to generate plasma. The first design explores a coaxial tube setup, and the second design entails a multi-hollow plate setup. This research was done in collaboration with TU Delft and the Dutch seed distribution company Bejo Zaden BV, and its main objective was to develop a sustainable and efficient alternative to conventional seed disinfection. The initial tube design used an acrylic tube as the dielectric and two stainless steel electrodes, but this design had some issues so a revised design with smaller dimensions was made to address these issues. The multi-hollow plate design used two steel electrodes with holes (with diameters ranging from $1 - 2.5mm$) and a dielectric made of polylactic acid. The experimental results showed that both setups work. In order to assess the final design, a program of requirements was made, which included requirements such as sustainability, safety, and scalability. Key findings suggest that the electrode and dielectric materials were not optimal, but were sufficient enough to prove the concepts. This study aims to advance the sustainable agricultural practices by providing an efficient plasma-based seed disinfection method. Future recommendations include optimizing electrode and dielectric materials and scaling the system for industrial use.

Preface

Bram van de Ruit & Teun Mertens
Delft, June 2025

We are pleased to present our thesis on the design and characterization of a low-temperature plasma reactor for seed treatment applications. This thesis is part of a larger group project called the bachelor graduation project of the faculty of Electrical Engineering at TU Delft. The project was carried out at the behest of Bejo Zaden BV, a global seed supplier based in The Netherlands. Current methods for seed treatments, such as a warm water bath, are not sustainable and take a long time, so Bejo Zaden reached out to TU Delft to help find a better solution to disinfect seeds. The goal of this project was to design and build a seed disinfection system suitable for commercial use. In order to achieve this our group divided the project into three parts: the high voltage power supply, the disinfection module & sensing, and the plasma generator. This thesis will contain the plasma generator part.

We couldn't have done this project alone and therefore we would like to express our gratitude to our supervisors. First we want to thank Em. prof.dr.ir. Jan van Turnhout, who was always ready to help and who's incredible enthusiasm has motivated us to deliver the best work we could. Next we want to thank Dr.ing. Henk van Zeijl, for asking the questions we didn't think about and for helping us think like a real engineer. Additionally we would like to thank Drs. Luutzen Wymenga, who had already researched the plasma generation topic and therefore was a tremendous help whenever we were stuck. Aside from our supervisors we would also like to thank Dr. Mohamad Ghaffarian Niasar, who's knowledge of high voltage applications made it possible to safely test our setups. We also want to acknowledge our fellow students from the Mechanical Engineering faculty Andries Russchen, Damon de Groot and Iris Schelleman because they helped us whenever we didn't know something mechanical related. Last but not least, we want to thank Ir. Yvette Bakker who was our contact at Bejo Zaden BV. She showed us what it was like to work for a client and gave us valuable feedback during the presentations.

We as a subgroup are grateful for the opportunity we got, it was amazing to get some hands-on experience and it was interesting to learn so many things outside of our usual curriculum. This project was really interdisciplinary and taught us a lot about working together, this experience will be of tremendous value later down our career paths. We also want to credit our fellow teammates Aditya Sachar, Matteo Corradetti, Olivier Krugers Dagneaux and Timo Neef, they were a pleasure to work alongside with and without them this project wouldn't have been possible.

Contents

Abstract i

Preface ii

1 Introduction 1
- 1.1 Seed disinfection . . . 1
- 1.2 State of the art analysis . . . 1
- 1.3 Document structure . . . 2

2 Program of Requirements 3
- 2.1 Mandatory Requirements . . . 3
  - 2.1.1 The system must generate Cold Atmospheric Pressure Plasma (CAPP) . . . 3
  - 2.1.2 The system must achieve 90% microbial reduction per batch . . . 3
  - 2.1.3 The system must not get hotter than $40°$C . . . 3
  - 2.1.4 The system must comply with IEC 61010-1 safety standards . . . 3
  - 2.1.5 The system must be sustainable . . . 3
  - 2.1.6 The system must work in the voltage range of our power supply . . . 3
- 2.2 Trade-off Requirements . . . 4
  - 2.2.1 The system should have an energy efficiency of 80% . . . 4
  - 2.2.2 The system should be scalable . . . 4
  - 2.2.3 The plasma exposure time of the system should be adjustable . . . 4
  - 2.2.4 The system should be easily maintainable . . . 4

3 Plasma background 5
- 3.1 What is plasma . . . 5
- 3.2 Methods to create cold atmospheric plasma . . . 5
- 3.3 Why do we want it . . . 6

4 Plasma tube design 7
- 4.1 Initial tube design . . . 7
- 4.2 Revised tube setup . . . 9

5 Plasma tube analysis 10
- 5.1 COMSOL simulations . . . 10
  - 5.1.1 COMSOL simulation initial tube setup . . . 10
  - 5.1.2 COMSOL simulation initial tube setup . . . 11
- 5.2 Testing the setups . . . 11
- 5.3 Ozone concentration . . . 12
  - 5.3.1 Ozone concentration of the initial tube setup . . . 13
  - 5.3.2 Ozone concentration of the revised tube setup . . . 14
  - 5.3.3 Temperature measurement of the revised tube setup . . . 14
  - 5.3.4 Lissajous & current figures . . . 15

6 Plasma plate design 16

7 Plasma plate analysis 18
- 7.1 COMSOL simulations . . . 18
- 7.2 Testing the setup . . . 19
- 7.3 Ozone concentration . . . 19
  - 7.3.1 Temperature measurement . . . 19
  - 7.3.2 Lissajous figures . . . 20

8 Discussion of the results 21

9 Conclusions & Recommendations **23**

A Appendix A **26**

1

Introduction

1.1. Seed disinfection

Food safety and sustainable agriculture have become more and more important over the years. It has become essential to produce healthy crops as the world's population keeps growing and the environment keeps changing. One of the most important steps in guaranteeing healthy food is the disinfection of seeds. Since infected seeds can lead to a number of problems, such as lower germination rates, diseases, and even food poisoning. The current methods, such as chemical treatments, heat, and washing with water, are not up-to-date with today's norms since they are either not effective enough or because they cause harm to the environment and thus are not sustainable.

A promising new method has emerged for disinfecting seeds. This promising method uses cold atmospheric pressure plasma (CAPP) to disinfect seeds. CAPP has the ability to inactivate microorganisms without being harmful to the environment since it doesn't leave any chemical residues, and it can be broken down into harmless components like air and water after treatment. This makes it a safe and sustainable disinfection method. Plasma, often referred to as the "fourth state of matter", is an ionised gas containing reactive oxygen and nitrogen species (RONS). These RONS are believed to be the cause of the antimicrobial effects of CAPP. One of the most promising applications of CAPP is to use it to create plasma-activated water (PAW). PAW is water that has the inactivation properties of plasma, making it an effective method to disinfect seeds because it is scalable and can be made in a short amount of time.

1.2. State of the art analysis

One of the applications of plasma is called plasma-activated water (PAW). PAW can be created by exposing water directly to CAPP. A study by Oliveira. M, et al. [1] looked at the effects of PAW when treating foods. Multiple experiments have proven that PAW has antimicrobial properties. The reason why PAW has these properties is not fully clear yet but there seems to be an agreement that it is caused by the RONS present in PAW. There are two methods for the activation of water that are most widely used in the food industry, namely applying the discharge of plasma above the water surface, which is the most commonly used one, or carrying out the discharge of plasma beneath the water surface.

Than et al. [2] explored how the composition of plasma-activated water (PAW) changes with treatment time and how this affects the development of Lactuca sativa L. seeds. They found that treating water with plasma for 10 to 20 minutes produced the best results, creating the right balance of nitrate and hydrogen peroxide to boost seed water uptake, germination rates, and seedling growth. When the treatment times were longer, the seeds experienced stress, which ended up slowing down their development.

Rotondo et al. [3] investigated whether plasma-activated water (PAW) could be used to control bacteria and fungi. The longer the water was exposed to the plasma, the more reactive substances it contained, causing the pH to drop significantly. This made the PAW more efficient at inactivating microbes. The

microbes investigated in this study were the fungal pathogen Botrytis cinerea and two bacteria, Xanthomonas campestris pv. vesicatoria and Bacililus amyloliquefaciens. All three of these microbes are frequently associated with plans and plant products. The bacteria were almost completely inactivated after just a minute, while it took around three minutes to get a strong effect against the fungal spores. Their results showed that nitrites and hydrogen peroxide were especially important for stopping microbial growth. The authors highlighted that adjusting plasma settings like treatment time is crucial because different microbes respond differently.

Rathore et al. provides information on the effects of different electrode and dielectric choices on the properties of plasma produced by a dielectric barrier discharge plasma device [4]. The study found that the introduction of electrode knurling on the ground electrode significantly enhanced the properties of plasma activated water by increasing localized electric fields, which led to a higher plasma discharge power and improved physicochemical properties of the plasma activated water such as a lower pH and a higher concentration of RONS.

According to Waskow [5] SDBD required shorter exposure times due to its high plasma density relative to a gliding arc, a corona array and a downstream microwave plasma.

1.3. Document structure

The focus of this thesis will be on designing, developing, and evaluating an effective plasma system for PAW production. In addition, the plasma system will be analyzed and assessed to see its potential for seed disinfection, contributing to the progression of sustainable agriculture.

In Chapter 2 the desired requirements of the system will be specified. After that there will be some elaboration on the creation and effects of plasma in Chapter 3. Then Chapter 4 and 5 will focus on the design and analysis of the first setup namely a plasma tube system using DBD. The second setup will be covered in Chapter 6 and 7. After that, the results will be discussed in Chapter 8 and the conclusions and some recommendations will be given in Chapter 9.

2

Program of Requirements

In order to design and build a good seed treatment system it is important to know what the system needs to do. To assess this a program of requirements was made. Our PoR consists of two types of requirements namely mandatory and trade-off requirements. The PoR will be used to assess our design and final product.

2.1. Mandatory Requirements

Mandatory requirements define the operational capabilities and performance objectives of the system. They describe the tasks that the system must perform in order to be viable.

2.1.1. The system must generate Cold Atmospheric Pressure Plasma (CAPP)

This is the most basic functionality. In order to make the plasma-activated water (PAW), it is of essence to create plasma. CAPP is a partially ionized gas. It operates at temperatures near room temperatures (lower than or equal to $50°$C). This makes it safe for biological applications [6].

2.1.2. The system must achieve 90% microbial reduction per batch

The goal of the whole system is to disinfect vegetable seeds. In order to do this it is not only important to make PAW but also important to build a setup to effectively disinfect the seeds.

2.1.3. The system must not get hotter than $40°$C

It is important that the system does not damage the seeds. In order to ensure this, the aim will be to make the system not hotter than $40°$C.

2.1.4. The system must comply with IEC 61010-1 safety standards

The system will operate with high voltages and it will work in an environment where there are people nearby so it is of essence that the system is 100% safe. Thus the system must comply with IEC 61010-1 safety standards, meaning that all high-voltage components are enclosed in insulated casings. Furthermore, there should be no leaks when injecting the plasma into the water since the RONS can be hazardous so the system must have a seal integrity of 90% under operating conditions.

2.1.5. The system must be sustainable

The company (Bejo Zaden B.V.) wants a sustainable way to disinfect their seeds. So it is important that the system does not use too much energy or water. Therefore, the system must not consume more than $0.5kWh$ per batch and less than $2L$ of water per kg of seeds.

2.1.6. The system must work in the voltage range of our power supply

The power supply provided by our team generates an AC $20kHz$ pulse with a peak-to-peak voltage in the range of $0 - 10kV_{pp}$, so the system must function within that voltage range.

2.2. Trade-off Requirements

Trade-off requirements define the requirements that are desirable for an optimal system but are not mandatory. They can be used as a benchmark to see how optimized the system is. The more trade-off requirements the system meets the happier the clients will be.

2.2.1. The system should have an energy efficiency of 80%

In order to be sustainable and cost efficient it is important that the system uses the energy it gets effectively.

2.2.2. The system should be scalable

The system is meant for commercial use by a large company (Bejo Zaden B.V.), which means that it is necessary for the system to be scalable since they will want to apply the system to their large-scale seed production. Therefore, the design of the system should be able to accommodate batch sizes of up to $10kg$.

2.2.3. The plasma exposure time of the system should be adjustable

Time is of essence for the commercial use of our system so it is important that the company (Bejo Zaden B.V.) can change how long the seeds are exposed to the PAW, the longer the exposure time the more efficient but time is money so you don't want it to take too long. Therefore, the plasma exposure time should be adjustable between 1-20 minutes to balance the efficacy and throughput of the system.

2.2.4. The system should be easily maintainable

The components of the system will most likely become less efficient over time, so in order for the system to be useful to the company, it needs to be easily maintainable. This means that all components of the system should be replaceable in 30 minutes and without the use of specialized tools.

3

Plasma background

3.1. What is plasma

Plasma, often referred to as the ”fourth state of matter”, is an ionized gas that can be artificially created by applying strong electric fields to a gas, which ionizes the gas and creates a low-temperature plasma. Plasma is highly conductive and contains charged particles (e.g., OH, H_2O+, electrons, etc.), reactive species (e.g., reactive oxygen species [ROS]: OH, O_2, $^1O_2$ and reactive nitrogen species [RNS], NO, $ONOO$, etc.), excited molecules (e.g., excited O_2, N_2, etc.), and UV photons (e.g., vacuum UV, UVC, UVB, etc.) [7]. There are different types of plasma with the main differences being the temperature of the plasma. For this project, the required plasma is the so-called cold atmospheric pressure plasma (CAPP). This means that the plasma temperature is around room temperature and that it can be created and sustained in normal ambient pressure environments. The first plasma generator design was made by Werner von Siemens and the drawing of that design can be seen in fig 3.1. The methods to generate plasma have evolved a lot since then and the modern methods will be explained in the next section.

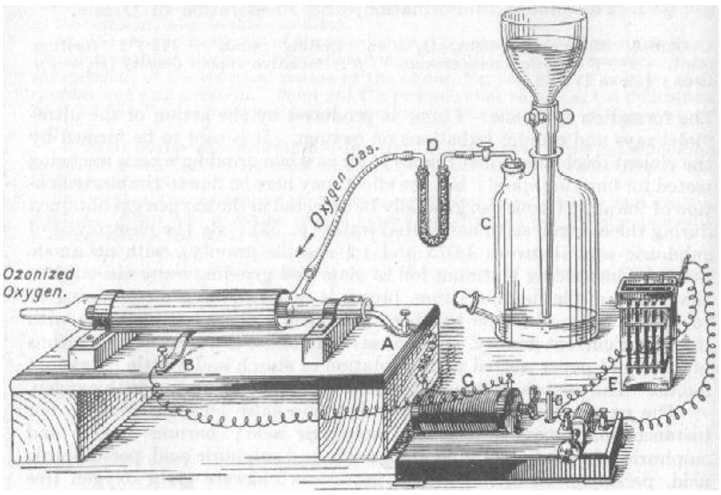

Figure 3.1: Ozone generator proposed by Werner von Siemens [Poggendorfs Ann. Phys. Chem. 102 (1857)]. [8]

3.2. Methods to create cold atmospheric plasma

As mentioned above, plasma can be artificially created by applying strong varying electric fields to a gas which causes electron collisions. In order to generate these varying electric fields an AC high voltage source will be used. There are several ways to create CAPP from various gases such as [6]:

- Dielectric barrier discharge (DBD)

- Plasma jet
- Corona discharge
- Gliding arc discharge

There are several gases that can be used to create plasma, with the most common ones being air, oxygen, nitrogen, helium, argon and their mixtures [9, 10, 11, 12]. The most commonly used method is dielectric barrier discharge (DBD). This method makes use of a high voltage source by applying this high voltage (kV) at high frequency (kHz) to two electrodes separated by a dielectric material. Plasma jets use two concentric cylindrical electrodes, where the inner electrode is connected to a high frequency power source. Corona discharge makes use of two or more sharp electrodes (usually something sharp like a needle or thin wire) and between these two electrodes high voltage will be applied generating an ionization process. Corona discharges have low electron and ion densities. Gliding arc discharge normally produces hot plasma, but under the right conditions it can also produce cold plasma. It uses electrodes placed in a fast gas flow [6]. Figure 3.2 shows these different methods. The method used in this thesis is DBD, this is because it is the most effective and cost-efficient to make.

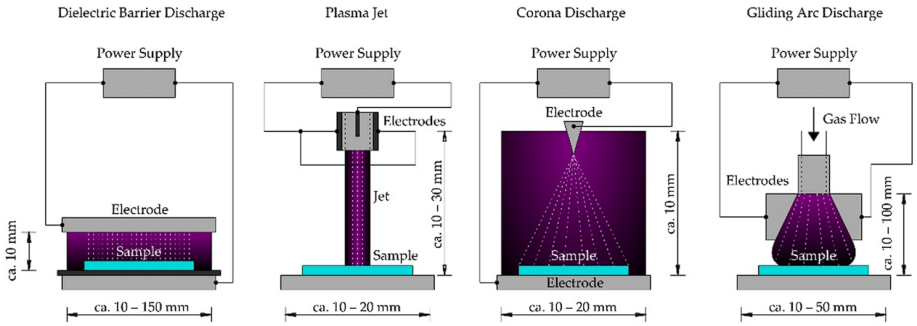

Figure 3.2: Schematic drawing of diverse cold atmospheric pressure plasma devices. [6]

3.3. Why do we want it

So why is CAPP wanted? CAPP contains RONS and ozone and these RONS and ozone are believed to contain antimicrobial properties, which makes it useful for disinfecting things (in the case of this thesis it will be used to disinfect vegetable seeds). Furthermore, a study on the effect cold plasma treatment on Korean ginseng seeds [13] has shown that it can also improve the germination rate and the fungicidal and bactericidal effects of the seeds. This study showed that cold plasma treatment can increase crop yield and shorten harvesting time because of this increased germination.

For this thesis, the main goal is to disinfect vegetable seeds; the way this will be achieved is by using plasma-activated water (PAW). The way PAW is created is by exposing water directly to CAPP [1], which is usually done by using a Venturi tube. PAW has the same antimicrobial properties as CAPP, but it has the advantage of being better distributable since water can be used in many forms. The inactivation efficacy of PAW is increased when either the plasma activation time or the bacterial incubation time is increased. It also showed that PAW has a greater inactivation effectiveness against gram-positive bacteria than gram-negative bacteria. As expected it was found that the inactivation efficacy deteriorates over time and this is affected by storage duration and temperature, where the longer and warmer you store it the less efficient it will become [14].

4

Plasma tube design

4.1. Initial tube design

For the first plasma generator design, the decision was made to design and build a tube DBD setup. The tube contains a bar that acts as an electrode, and the second electrode is a mesh that is wrapped around the outside of the tube. The tube design makes it easier to funnel the plasma into the Venturi tube which makes the PAW making process more efficient.

There are quite a lot of suitable dielectric materials that can be used for DBD such as:

- Alumina
- Quartz
- Glass
- Borosilicate glass
- Teflon
- Acrylic

Each of these materials has its own advantages and disadvantages. In view of the budget and time duration of this project, the decision was made to make the first design using acrylic (PMMA). Acrylic has a high enough dielectric strength that makes it suitable for high voltage applications such as DBD. Acrylic is not the most optimal material because its dielectric strength is not the best compared to some of these other materials. The dielectric strength of acrylic is around $30kV/mm$ while the other materials have dielectric strengths of: alumina ($16.7kV/mm$), quartz ($30kV/mm$), glass ($40kV/mm$), borosilicate glass ($34kV/mm$), teflon ($80kV/mm$) [15, 16, 17, 18, 19, 20]. Even though some of the materials like alumina and quartz have equal or lower dielectric strengths, they are still more efficient due to their better thermal conductivities and thermal stability (the thermal conductivity of alumina is $18W/m-K$, quartz $1.38W/m-K$, while for acrylic it is $0.19W/m-K$). However, acrylic has the benefit of being cheap and easy to make, which means that it is a great material if time is short and money is low.

For the electrodes, there are also a lot of materials suitable for generating CAPP:

- Stainless steel
- Aluminum
- Copper
- Titanium
- Metal meshes

For the tube design the decision was made to use a stainless steel bar for the inner electrode and a brass mesh. Again, this decision was made due to the budget and time duration of this project.

The thickness of the acrylic tube is $3mm$, and the gap between the stainless steel bar and the brass mesh is around $22mm$. The decision was made to use a second acrylic tube to hold the mesh in place. The inner tube has a diameter of $60mm$ and the outer tube has a diameter of $70mm$, and both tubes have a length of $320mm$. A schematic of this setup can be seen below in Fig. 4.1.

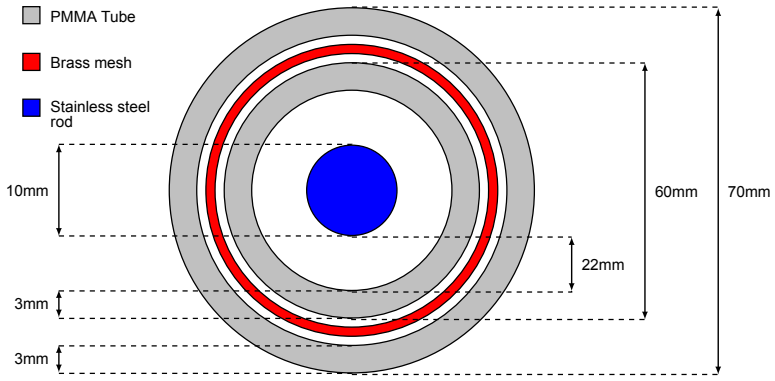

Figure 4.1: Initial tube schematic

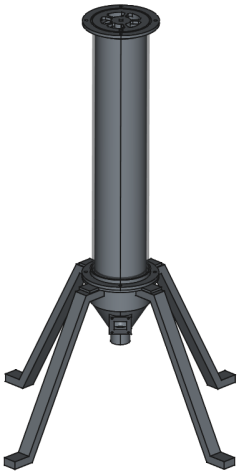

(a) FreeCAD 3D design of the whole tube setup

Figure 4.2: 3D designs of the ozone tube components

To hold the whole system in place without touching it, a $3D$ tube clamp nozzle (TCN) was designed; the design of that TCN can be seen in Fig. 4.2. In the design, it can be seen that the tube is held in place with two caps, one of them extends into a nozzle, which makes it suitable for connecting to the Venturi tube. The decision was made to make the tube stand vertically since this will ensure better flow of the plasma into the Venturi tube. Four legs were designed to hold the tube upright. After the 3D design was completed, it was printed using polylactic acid (PLA), which is a polyester made from renewable biomass [21].

The final built tube setup can be seen in Fig. 4.3. The high voltage source will be connected to the stainless steel ba,r and the mesh, and air will flow through the tube acting as the working gas. In Fig. 4.3, there is also a green PCB visible; this is the ozone sensor that measures the amount of ozone (O_3). The reason why the amount of ozone is important is that ozone is a strong oxidant [22]. This means that ozone can oxidise the organic molecules contained in the cell membrane, which effectively kills the unwanted microbial organisms [23]. Therefore, the greater the amount of ozone present in the plasma, the more effective the disinfection setup will be. The results of the ozone sensor and an in-depth analysis of the operation of the tube plasma generator will be covered in the next chapter.

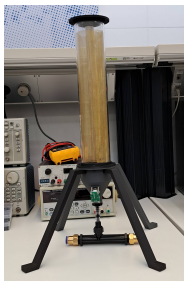

Figure 4.3: Initial tube setup

4.2. Revised tube setup

The first tube design had a few issues, the main issue being the distance between the two electrodes and the thickness of the dielectric (namely $3mm$). This is the reason why the initial setup did not work, since the amount of voltage required to generate plasma was too high. To address this problem, the decision was made to buy new tubes with a smaller diameter and with a smaller thickness. The new inner tube has a diameter of $7mm$ and the outer tube has a diameter of $11mm$, each tube having a length of $15cm$. The thickness of the new tubes is $1mm$, making it 3x thinner than the initial tubes. A schematic of this setup can be seen in Fig. 4.5. Furthermore, the decision was made to change the stainless steel bar into a handmade spring with a diameter of approximately $5mm$ made of tinned copper wire (diameter $0.71mm$) . For the outer electrode, the same mesh was used as in the initial design. The old 3D design of the TCN (Fig. 4.1a) was slightly altered to fit the new tubes. This new 3D design can be seen in fig 4.4.

Figure 4.4: 3D design of the new TCN

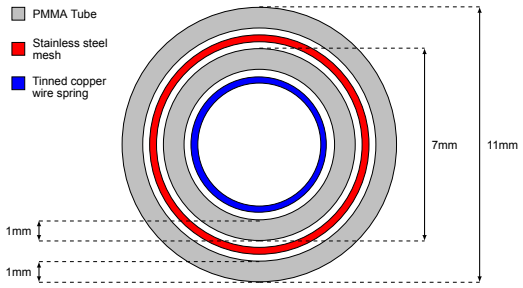

Figure 4.5: Small tube schematic

In order to improve the efficiency, the decision was made to put three tubes in parallel, this means that the power supply should supply a higher voltage but will also increase the plasma output of the setup. The new tubes can be seen in fig 4.6. An air pump was also added at the bottom of the TCN, which ensured good flow of the ozone.

Figure 4.6: Photo of the revised tube setup

5

Plasma tube analysis

5.1. COMSOL simulations

To analyze the electric fields produced by the plasma sources, the setups were modeled using the physics simulation software COMSOL Multiphysics. These simulations provide valuable insights into the behaviour and characteristics of the plasma sources. However, it is important to note that such models are simplifications and do not fully capture the complexities of real-world plasma dynamics. Various effects and interactions are not accounted for in a basic COMSOL setup, so the results should be interpreted accordingly.

5.1.1. COMSOL simulation initial tube setup

In Fig. 5.1, the simulated electric field of the initial tube setup can be seen. As can be seen in the plot, the magnitude of the electric field falls below the required breakdown voltage of air $3 \times 10^6 V/m$ and should most likely fail to produce plasma while staying within the voltage requirements as stipulated in 2.1.6.

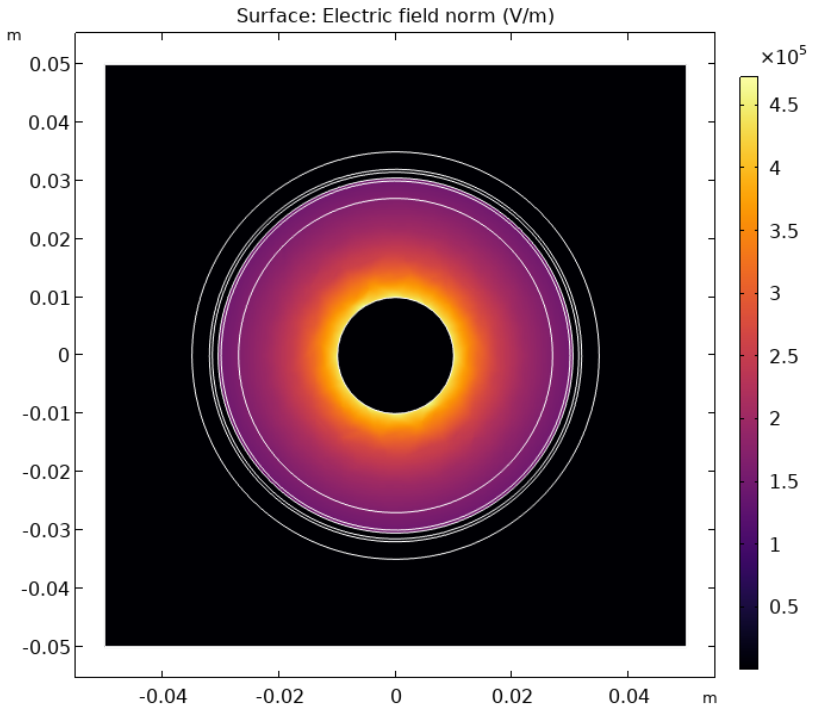

Figure 5.1: Electric field simulation of the tube setup

5.1.2. COMSOL simulation initial tube setup

The simulated electric field for the revised tube setup can be seen in Fig. 5.2. Here, the simulated electric field does breach the $3 \times 10^6 V/m$ breakdown voltage of air and should succeed in producing plasma. Further in this plot, small pockets of high electric field magnitudes can be seen close to the spring. This is, however, in large part due to COMSOL reducing the smooth circular wire used for the spring into a mesh containing many sharp angles, which does not represent reality.

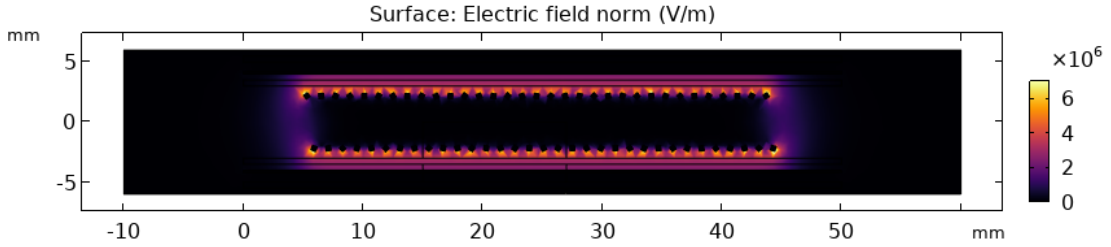

Figure 5.2: Electric field simulation of the revised tube setup

5.2. Testing the setups

To test the setups, a 50Hz high-voltage source was used. A circuit representation of the test setup can be seen in Fig. 5.3 The equivalent circuit of the DBD electrodes has been adapted from [24]. In this equivalent circuit:

- C_g and R_g represent the capacitance and resistance of the air gap between the electrode surfaces and the dielectric barrier.
- C_d represents the capacitance of the dielectric barrier.
- C_{ref} is the reference capacitor used for charge measurement

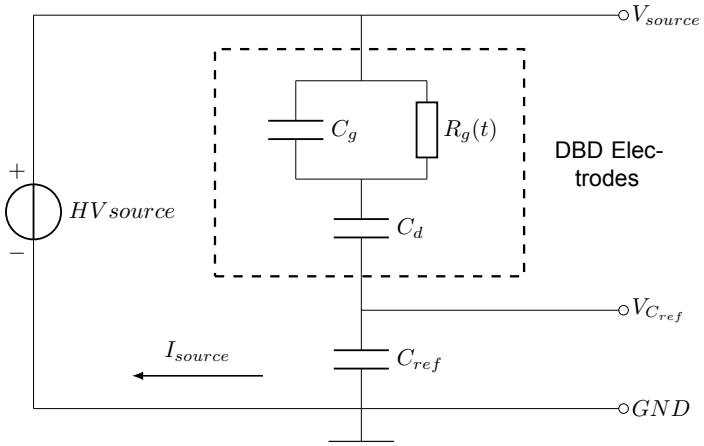

Figure 5.3: Test setup equivalent circuit

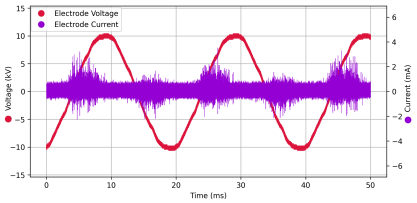

Figure 5.4: Example current plot

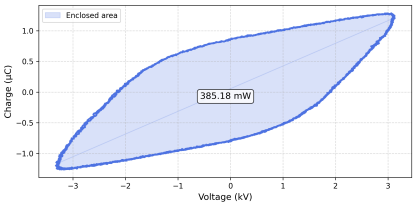

Figure 5.5: Example Lissajous plot

In Fig. 5.4 an example plot is shown of the current I_{source} and the applied voltage V_{source} where the periodic groupings of small peaks in the current show micro discharges in the plasma [25] which occur when the voltage across the electrode reaches a threshold value where discharges can occur.

To determine the total power injected into the plasma, the charge on the electrode must be known. For this purpose, the capacitor C_{ref} was connected between the electrodes and ground. This capacitance was selected to be approximately $100x$ the system's total capacitance, which was $87.5pF$, since this would ensure accurate charge measurements. If the capacitance was too small, then the voltage drop would be significant which would reduce the actual voltage applied to the plasma generator. Due to

charge neutrality in a series circuit, the charge on C_{ref} is equal to the charge on the electrode. The instantaneous charge on the electrodes is determined using the following formula:

$$Q_{Electrodes} = C_{ref} \cdot V_{C_{ref}} \tag{5.1}$$

This information was used to construct Lissajous figures where charge is plotted against the voltage, an example of which can be seen in Fig. 5.5. These Lissajous figures give insight into the plasma behaviour, where the area enclosed by the loop represents the energy consumed during one period, with the power being obtained by multiplying the energy by the applied excitation frequency($50Hz$). This, however, is not exclusively the power injected into the plasma, but all real power dissipated, so it includes ohmic losses [24]. The creation of these figures and the calculation of the surface enclosed by the Lissajous curve were done in Python. The code used can be seen in Appendix A.1 and A.2.

The tests were conducted in the ESP lab of TU Delft to ensure safe handling of high voltages. The setup for the initial tube test is shown in Fig. A.2 in the appendix. A high-voltage probe was used to measure the voltage across the electrodes. During the test of the initial tube setup, no plasma discharge was observed—there was no characteristic purple glow or notable ozone smell.

Interestingly, when the applied voltage reached $7.5kV$, an arc was observed. This arc burned through the stainless-steel mesh surrounding the outer part of the inner tube, indicating electrical breakdown without effective dielectric barrier discharge.

5.3. Ozone concentration

Ozone acts as a disinfection agent as mentioned in chapter 4, so for small amounts of ozone, it is generally true that more ozone means better disinfection. However, a study on the impact of ozone treatment on seed germination has shown that too much ozone is bad for seed germination [26]. This means that there should be enough ozone present to act as an effective disinfection agent but not too much, because otherwise it will have negative consequences for the seeds. Thus, it is important to know how much ozone is present.

The ozone sensor used is the DFRobot Gravity Ozone Sensor. An image of this sensor can be seen in fig 5.6. This sensor has a measurement range of 0-10 ppm with a resolution of 0.01 ppm (10 ppb) [27]. It uses Inter-Integrated Circuit, widely known as the IIC protocol, which makes it compatible with many microcontrollers such as the ESP32-s3 [28] series, which is the microcontroller that was used during the measurements of the system. For calibration of the sensor, the sensor was used to measure the amount of ozone in the air, which is around 0-1 ppb, as can be seen in fig 5.7. The setup used for the calibration can be seen in fig A.1.

Figure 5.6: DFRobot Gravity IIC Ozone Sensor (0–10 ppm), model SEN0321. Image from [29].

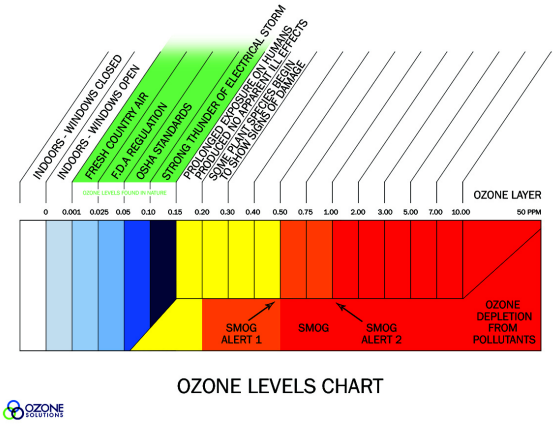

Figure 5.7: Reference chart of ozone exposure levels. Adapted from [30].

The data from the ozone sensor was read by making use of the ESP32-s3 microcontroller. The ESP

board sent the data to a server where the measurements were stored. To make it easy to read, a simple dashboard was created using Excel; a screenshot of this dashboard can be seen in Fig. A.4. During the calibration test, the sensor measured around 70-150 ppb. This value is too high compared to the 0-1 ppb that should be measured, which means that the sensor is not fully accurate.

5.3.1. Ozone concentration of the initial tube setup

The graph of the ozone measurements with the initial tube setup can be seen in Fig. 5.8, where the x-axis shows the time and the y-axis shows the ozone concentration in ppb. There were some unusual points during the measurements where the ozone concentration dropped to 0, even though the power supply was still active. These inconsistencies are likely due to a technical error of the sensor itself and will therefore be ignored. The graph shows that the maximum achieved ozone concentration was about 125 ppb, which is within the ozone concentration range of normal room air measured during the calibration, which means that the initial tube setup did not produce any ozone, and thus failed to generate plasma.

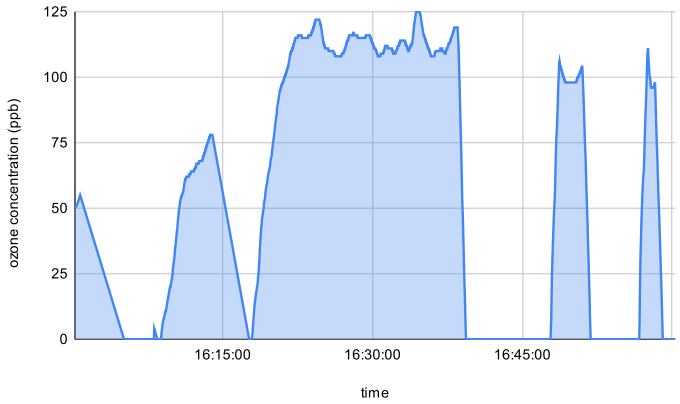

Figure 5.8: Graph of the ozone concentration during the measurements of the initial tube setup

5.3.2. Ozone concentration of the revised tube setup

For the ozone measurement of the revised tube setup, a different setup was used, which can be seen in Fig. A.3. This setup makes use of a different high voltage source, but the principle idea stays the same. For the ozone measurement a different ozone meter was used, because the DFRobot sensor could only measure up to 10 ppm, which was too low. The used ozone meter was the SKY2000-WH-O3 [31], which has a range from 0-5000 ppm. The ozone concentration of the revised tube setup was tested in two laps of 5 minutes each, once with the air pump on and once without. For the one without the temperature of the setup was also measured over time. The results of this can be seen in table 5.1a and table 5.1b. Furthermore, to test the seal integrity, the air outside of the setup was also tested, but no amount of ozone could be detected. It is important to note that the power supply used was supplying a $50Hz$, and a higher frequency would likely cause a higher ozone concentration. The measurements show that the setup can supply a stable ozone supply, which is convenient since the setup would need to be able to supply plasma for a longer period of time when used commercially.

Time (min)	O_3 (ppm)
0	0
1	40
2	55
3	60
4	64
5	64

(a) Pump on

Time (min)	O_3 (ppm)	Temp (°C)
0	0	25.6
1	18	25.6
2	23	25.7
3	30	25.8
4	24	25.8
5	26	25.8

(b) Pump off

Table 5.1: Ozone concentration over time with and without the pump.

5.3.3. Temperature measurement of the revised tube setup

An infrared thermometer was used to measure temperature. Specifically, the Fluke 568 Infrared-thermometer, which has a temperature resolution of $0.1°$C [32]. The measured temperature was $24.3°$C. This can be seen in Fig. 5.9.

Figure 5.9: Photo of the temperature measurement of the revised tube setup

5.3.4. Lissajous & current figures

Finally, the test setup explained in 5.2 was used to create the current and Lissajous figures and find the power dissipated in the setup. Below in Fig. 5.10, a plot of the current I_{source} and the applied voltage V_{source} can be seen. Clear spikes in the current can be seen with a rising and falling voltage, confirming the creation of plasma.

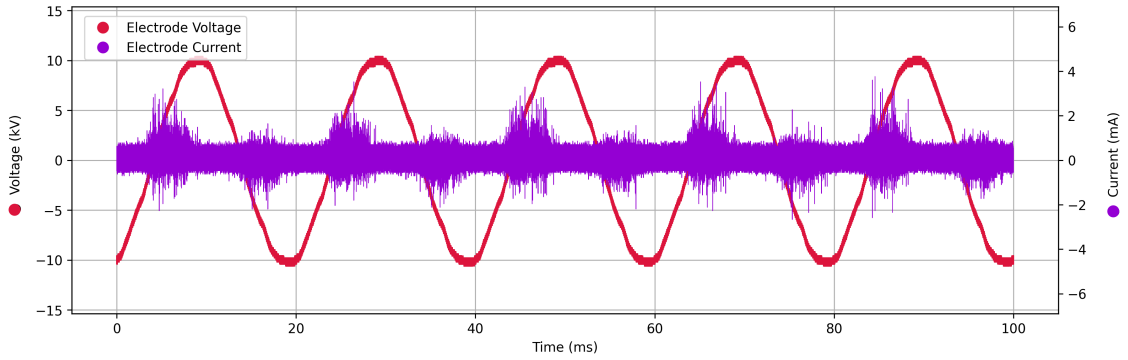

Figure 5.10: Electric current in the revised tube setup under a $10kV$ $50Hz$ excitation

In Fig. 5.11, four Lissajous figures can be seen, each showing the result for a different excitation voltage. It can be seen that as the voltage rises, the plotted loop opens up. In Fig. 5.11a, it can be seen that the Lissajous figure is almost closed, which means that this is the threshold voltage above which the tube setup will begin generating plasma.

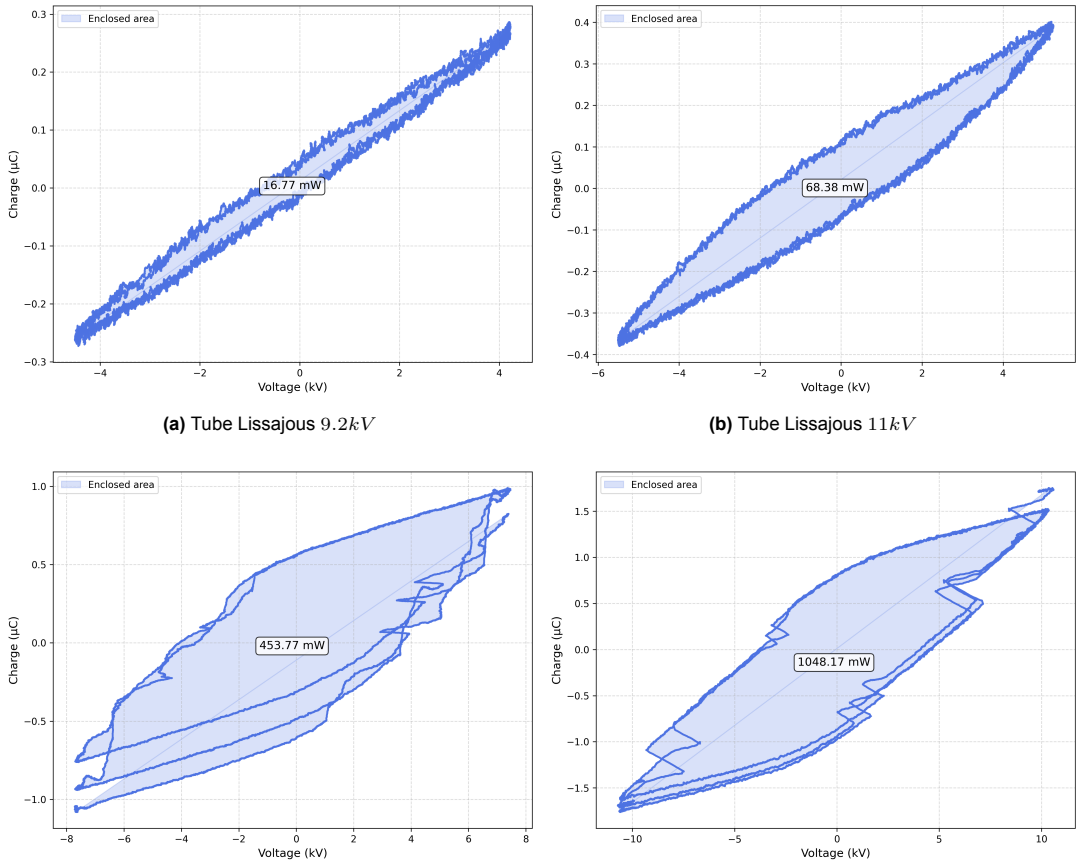

(a) Tube Lissajous $9.2kV$

(b) Tube Lissajous $11kV$

(c) Tube Lissajous $15kV$

(d) Tube Lissajous $21kV$

Figure 5.11: Lissajous figures of the coaxial tube setup

6

Plasma plate design

For the second plasma generator design, the decision was made to design and build a multi-hollow plate DBD setup. This idea came up in another BSc-thesis from TU Delft [33]. The method uses two electrode plates with a dielectric plate between them. This in itself is a fairly common method for generating plasma, but the twist is that the electrodes and the dielectric have a lot of small holes in them. A 3D design of one of these electrodes can be seen in fig 6.2.

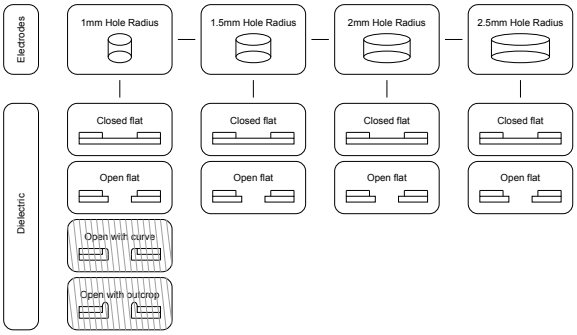

Figure 6.1: MHDBD options

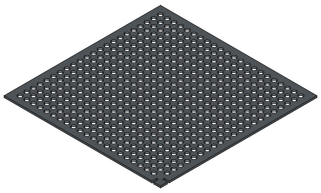

Figure 6.2: 3D model of a multi-hollow plate electrode with holes of a diameter of 1.5mm

Several different options for the dielectric were considered, designed and simulated, Simple illustrations of the different electrode and dielectric options considered can be seen below in Fig. 6.1, the options that were not able to be produced in time are shaded.

A study done by Cimerman et al. [34] looked at the production of gaseous species using a multi-hollow setup. According to the study, the reason why this method is effective is that the unique geometry forces the carrier gas to pass through the holes (hollows) where the discharge is generated. When high voltage is applied to this setup, the discharge will form on the edges of each of the holes. The time of gas within the active plasma region gets maximised since the air passes directly through the holes. This makes the generation of the RONS more effective. The study concluded that the production yield of ozone when using the multi-hollow setup is higher than that of other surface dielectric barrier discharge-based plasma generators. Here, the production yield (PY) is calculated using the following formula:

$$\mathrm{PY}(\ \mathrm{g/kWh}) = \frac{\text{Mass of } \mathrm{O_3} \text{ produced}}{\text{Energy input}} = \frac{c \cdot Q}{P} \tag{6.1}$$

Another benefit of this setup is that it is simple, which makes it easily scalable and thus makes it a great method for companies such as Bejo Zaden BV. However, the multi-hollow setups produced in the

study by Cimerman et al. [34] have both electrodes fully encased in a ceramic material so that there is no direct path through the air between the electrodes. Reproducing this setup would be challenging and costly, so in an attempt to imitate this setup, different dielectric options were considered. Seen in Fig. 6.5 and in Fig. 6.1 under ”Open with curve” and ”Open with Outcrop”, are two options where a dielectric wall is inserted into the holes, further separating the two electrodes. However, due to time constraints, it was not feasible to make them within the time limit, and therefore, the decision was made to use flat dielectrics with normal holes in them.

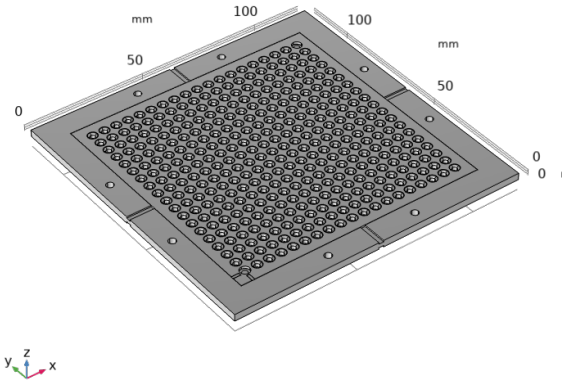

Figure 6.3: Open dielectric design with curved hole walls

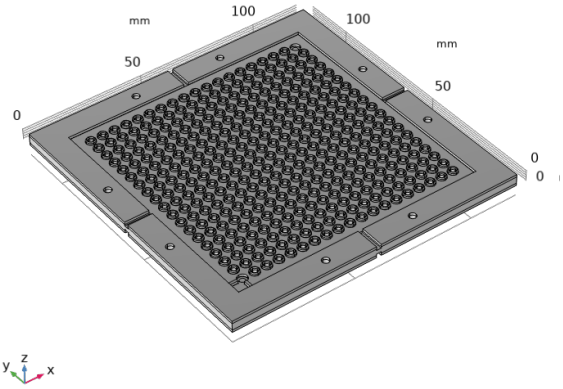

Figure 6.4: Open dielectric design with outcropped curved hole walls

Figure 6.5: Dielectric designs with walled holes

Four pairs of multi-hollow electrodes and dielectrics were made using the 3D design seen in fig 6.2. The dielectrics were 3D printed and are made of PLA. The electrodes were made by cutting holes in a 100x100mm steel plate with a Lion Alpha Metal laser cutter [35]. The plates have different sizes of holes, with diameters of 1mm, 1.5mm, 2mm, 2.5mm. The electrodes can be seen in fig 6.6

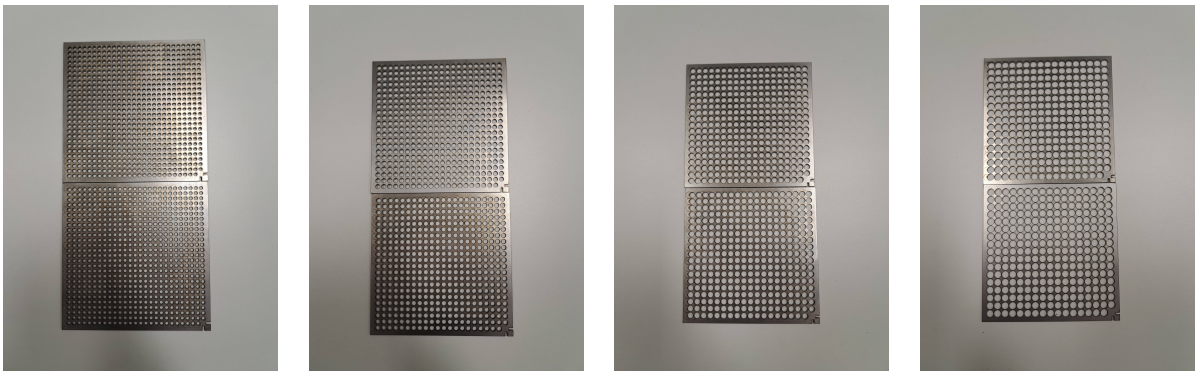

(a) 1mm (27×27) **(b)** 1.5mm (22×22) **(c)** 2mm (19×19) **(d)** 2.5mm (17×17)

Figure 6.6: Multi-hollow plate electrodes with various hole diameters and corresponding hole matrices.

7

Plasma plate analysis

7.1. COMSOL simulations

Again for the analysis of the electric field produced by the plasma plates COMSOL Multiphysics was used the results of which, using a DC excitation of 5kV, can be seen below in Fig. 7.1.

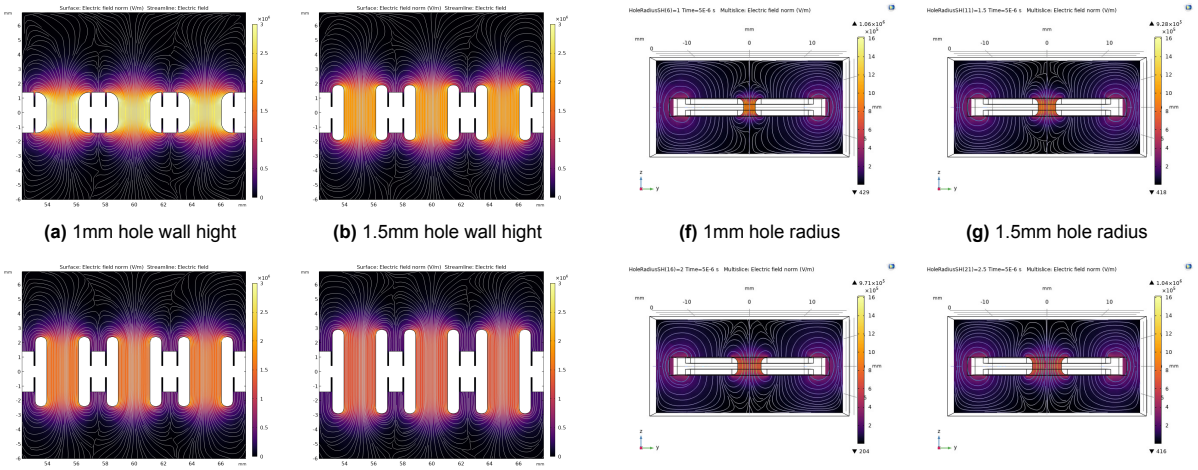

(a) 1mm hole wall hight **(b)** 1.5mm hole wall hight **(f)** 1mm hole radius **(g)** 1.5mm hole radius

(c) 2mm hole wall hight **(d)** 2.5mm hole wall hight **(h)** 2mm hole radius **(i)** 2.5mm hole radius

(e) Simulated multi-hollow electrodes with varying hole wall heights **(j)** Simulated multi-hollow electrodes with varying hole radii

Figure 7.1: Comparison between simulated and photographed multi-hollow electrode plates.

The results shown in Fig. 7.1e depict the behaviour of the electric field when increasing the height of the dielectric wall present in the hole. It can be seen in 7.1a that the electric field reaches above the breakdown voltage of air ($3 \times 10^6 V/m$) while the others sit below it, however this set up carries a risk. As there is a direct path from plate to plate though the air in this setup arcs will be quick to form the dielectric walls present in the holes serve to lessen that behavior. The intention is that adding a frequency component to the excitation would increase the electric field where the plates are closest to each other.

In Fig. 7.1j the simulated results with different hole radii can be seen. Designing for a uniform electric field within the hole a smaller hole radius is clearly more optimal as a significant drop in the electric field magnitude can be seen at the center of the hole for larger hole radii. However that is not the only consideration as the manufacturing of small details, as are required for the dielectric hole walls, are challenging to realize.

7.2. Testing the setup

The plasma plate setup was also tested in the ESP lab. The 3D design of the plasma plate was a little bit too small which meant that the plates had to be tested without the box surrounding them. This made it less safe but it is an issue that can quickly be fixed by updating the 3D design so it won't affect the final performance of the setup. A different issue however was that the dielectric was too thick and did not work. The reason why it didn't work was because the voltage needed to create partial discharge was so high that it would cause arcs. These arcs between the and the electrodes were caused due to the dielectric acting as an open connection at voltages that were too high, which made it unusable. In order to fix this, a different dielectric was used without holes in it. This dielectric was made of aluminium oxide (Al_2O_3) and had a thickness of $0.6mm$. This change of the dielectric made it work and thus all the measurements were done with this dielectric and not with the 3D printed ones.

7.3. Ozone concentration

For the plasma plate setup, the same measurement methods were used as for the revised tube setups mentioned in chapter 5. However as mentioned earlier, the 3D design didn't fit which meant that there was no airtight connection to the TCN and therefore it was not possible to measure the ozone concentration with the ozone meter. However, the distinct smell of ozone was noticeable in the air surrounding the setup which is an indicator of it working correctly.

7.3.1. Temperature measurement

For the temperature measurements of the plate the same infrared thermometer was used. The temperature was measured for the $1mm$ plate and for the $2.5mm$ plate. The temperature of the $1mm$ plate was $24.8°$C and for the $2.5mm$ plate it was $30.8°$C indicating a rise as the holes get bigger. The measurements can be seen in fig 7.2.

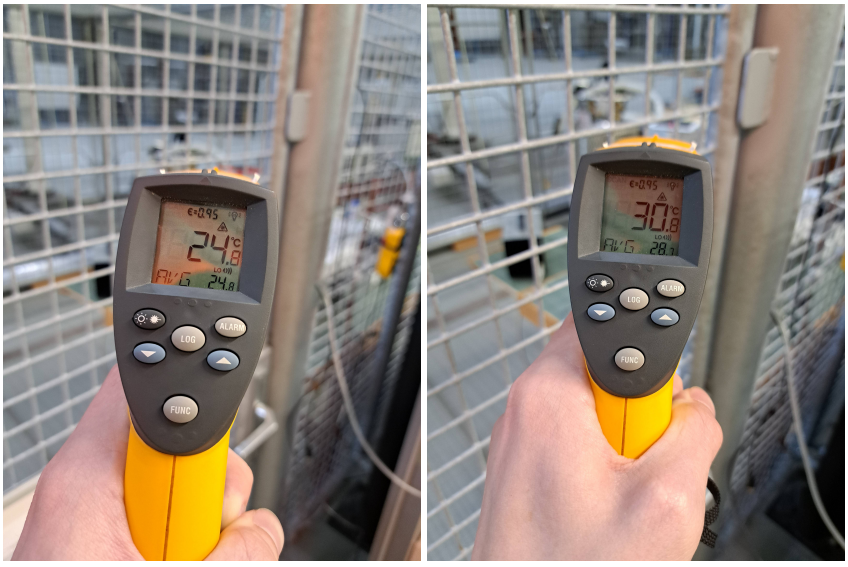

(a) Temperature measurement of the $1mm$ plate **(b)** Temperature measurement of the $2.5mm$ plate

Figure 7.2: Temperature measurements of the multi-hollow plates

7.3.2. Lissajous figures

To find the power injected into the plasma the same method was used as mentioned in 5. Again, the loops are seen to be open, and so power is being dissipated in the setup, indicating plasma generation.

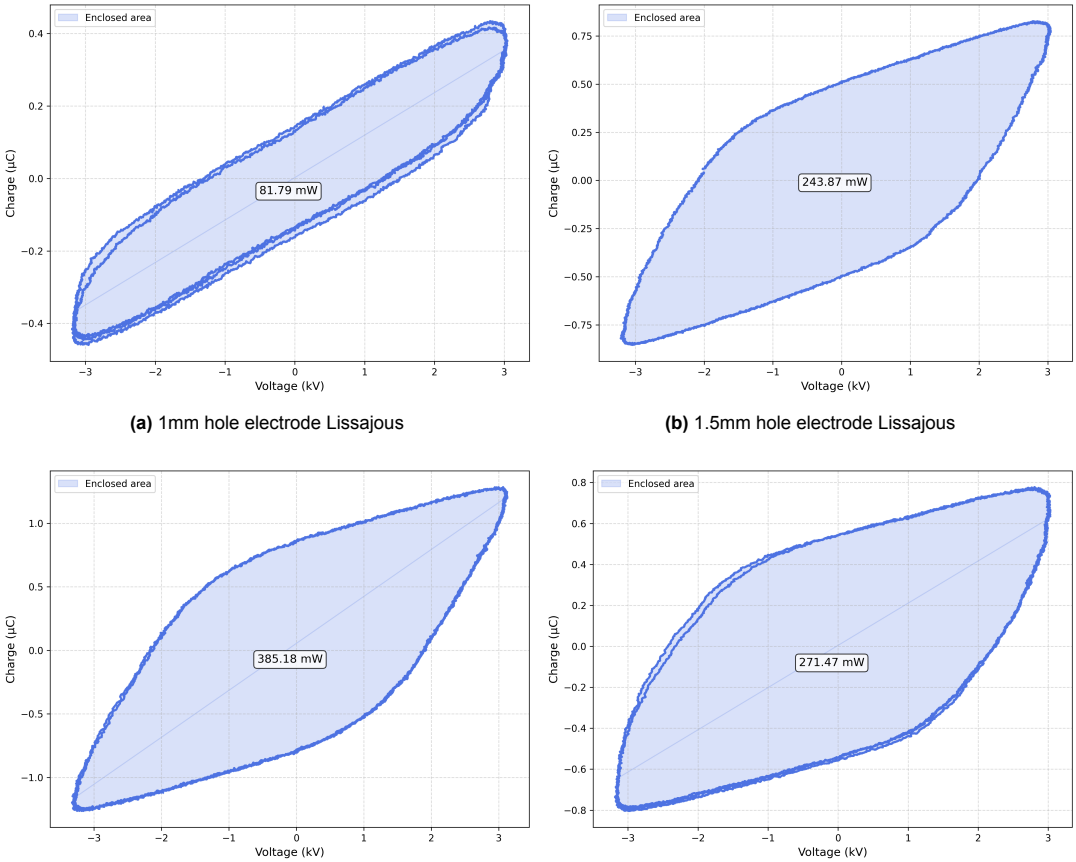

(a) 1mm hole electrode Lissajous

(b) 1.5mm hole electrode Lissajous

(c) 2mm hole electrode Lissajous

(d) 2.5mm hole electrode Lissajous

Figure 7.3: Lissajous figures of the plasma plates.

8

Discussion of the results

The results of this study show that both the revised tube setup as well as the multi-hollow plasma plates are viable plasma sources; however, it is important to note that only ozone was measured, so the effectiveness of the RONS and other particles is unclear. The initial tube design did not work since the dielectric was too thick and there was too much space between the electrodes, but the revised design with the smaller tubes proved that the concept of the tubes works.

The ozone measurements proved that plasma was generated and this means that CAPP was successfully generated, so the first requirement is achieved. The second requirement was about the microbial reduction, but since the seeds weren't tested in time, there is no way to determine if this requirement was achieved. The third requirement stated that the system should not get any hotter than $40°$C since that would harm the seeds. The infrared thermometer showed that the maximum temperature of the tube setup was around $24.3°$C and of the plate setup around $30.8°$C, which means that the temperature requirement was fulfilled. The tube setup was encased in an acrylic tube, and the plate setups were encased in a 3D-printed PLA container, which means that both setups complied with the IEC 61010-1 safety standards. Since there was no ozone in the air around the setup, it is also safe to say that the 90% seal integrity under operating conditions was achieved.

The water used in the system can be recirculated, which makes it sustainable. As for the amount of kWh per batch, this mainly depends on the power supply which is outside of the scope of this study and thus the sustainability requirement will be marked as sufficient. Lastly, the system has to function with the voltage range of $0 - 10kV$, and this requirement was also fulfilled since the thresholds of the setups were below $10kV$. This means that almost all of the mandatory requirements were fulfilled.

As for the trade-off requirements: the energy efficiency was sadly not measured, the system is scalable, but it is uncertain if it is scalable to a size that would accommodate batch sizes of $10kg$, the plasma exposure time is adjustable, and the system consists of multiple smaller parts which makes it easily maintainable.

The measurement results of the initial coaxial tube setup were quite disappointing since it did not work, but it provided valuable insights into dielectric and electrode optimisation. However, this was to be expected, and the revised coaxial tube setup proved that the concept of the design works. The amount of ozone produced was good given the fact that a voltage signal of only $50Hz$ was used. The tube setup started working from $9.2kV_{pp}$, which means that an amplitude of $4.6kV$ is needed to generate plasma with this setup. This is quite a high voltage, and it would be better and more efficient to make this threshold voltage a little lower. This could be achieved by using different electrode and dielectric materials. A quick way to improve the setup is to use higher-quality springs made of a better electrode material (such as tungsten) than the hand-made springs that were used in the tested setup. Furthermore, the dielectric tubes were made of acrylic, which is also far from the best; a better material for the dielectric would be something like quartz or borosilicate glass (both of which are way more expensive than acrylic).

The final multi-hollow plate setup was not exactly as designed since the original design of the dielectric plates had outcropping holes on them, which means that the results of that design remain unclear. The measurement results of the multi-hollow plasma plate setup were promising, but it is important to note that the test setup was not ideal and therefore it wasn't possible to accurately measure the amount of ozone produced or the threshold voltage of the plate setup. However, the distinct smell of ozone was present above the plates after testing, which indicates that the concept worked, although it is uncertain how well it worked. More scientific proof is the Lissajous figures, which showed that there were in fact partial discharges which indicates that plasma was generated.

9

Conclusions & Recommendations

The goal of this work was to design and characterise a low-temperature plasma reactor for seed treatment applications. During the project, two low-temperature plasma reactor setups were designed: a coaxial tube design and a multi-hollow plate design, both using DBD. Both setups demonstrated the ability to create CAPP and produce ozone, which means that the primary requirement of the project has been fulfilled. The revised tube setup showed that it can produce a stable amount of plasma and the multi-hollow plate setup also showed its ability to generate plasma without getting too hot, even though this required a change of the dielectric. The interdisciplinary collaboration between TU Delft and Bejo Zaden BV proved the practical viability of plasma-based seed disinfection as a sustainable alternative to conventional methods.

The results were satisfactory for the limited time of this study; however, there is still a lot left to do regarding this topic. For future work it would be good to look at different materials for the electrodes and dielectrics, which can make the setups way more efficient. Another thing that this study did not manage to look at is how to make the system scalable for commercial use, which is also something that could be looked at. Furthermore, the tests that were run on the setups didn't fully mimic the industrial environment in which it would operate when used commercially, so more advanced tests should be run. These tests could study how well the setups work when used for a longer period (the maximum time it was used now was around 10 minutes). Another thing that could be studied in future work is to make the dielectric plates with outcropped holes, like they were originally designed. And something that is even more important is that the setup should be tested on its microbial reduction efficacy, since this wasn't done during this study due to time constraints.

Bibliography

[1] M. Oliveira, P. Fernández-Gómez, A. Álvarez-Ordóñez, M. Prieto, and M. López, "Plasma-activated water: A cutting-edge technology driving innovation in the food industry," *Food Research International*, vol. 156, p. 111368, 6 2022.

[2] H. A. Q. Than, T. H. Pham, D. K. V. Nguyen, T. H. Pham, and A. Khacef, "Non-thermal plasma activated water for increasing germination and plant growth of lactuca sativa l," *Plasma Chemistry and Plasma Processing*, vol. 42, pp. 73–89, 1 2022.

[3] P. R. Rotondo, D. Aceto, M. Ambrico, A. M. Stellacci, F. Faretra, R. M. D. M. Angelini, and P. F. Ambrico, "Physicochemical properties of plasma-activated water and associated antimicrobial activity against fungi and bacteria," *Scientific reports*, vol. 15, p. 5536, 12 2025.

[4] V. Rathore and S. K. Nema, "Effects of electrodes surface texture, electrodes materials and dielectric material on properties of plasma activated water," *Physics Letters A*, vol. 524, p. 129831, 11 2024.

[5] A. Waskow, F. Avino, A. Howling, and I. Furno, "Entering the plasma agriculture field: An attempt to standardize protocols for plasma treatment of seeds," 2022.

[6] M. Domonkos, P. Tichá, J. Trejbal, P. Demo, and B.-G. Rusu, "Applications of Cold Atmospheric Pressure Plasma Technology in Medicine, Agriculture and Food Industry," 2021.

[7] N. Wannicke, R. Wagner, J. Stachowiak, T. M. Nishime, J. Ehlbeck, K. D. Weltmann, and H. Brust, "Efficiency of plasma-processed air for biological decontamination of crop seeds on the premise of unimpaired seed germination," *Plasma Processes and Polymers*, vol. 18, no. 1, 2021.

[8] W. Siemens, "Ueber die elektrostatische induction und die verzögerung des stroms in flaschendrähten," *Annalen der Physik*, vol. 178, no. 9, p. 66, 1857.

[9] K. Ollegott, P. Wirth, C. Oberste-Beulmann, P. Awakowicz, and M. Muhler, "Fundamental properties and applications of dielectric barrier discharges in plasma-catalytic processes at atmospheric pressure," *Chemie Ingenieur Technik*, vol. 92, no. 10, pp. 1542–1558, 2020.

[10] H. D. Stryczewska, "Supply systems of non-thermal plasma reactors: Construction review with examples of applications," *Applied Sciences*, vol. 10, no. 9, p. 3242, 2020.

[11] M. Izadjoo, S. Zack, H. Kim, and J. Skiba, "Medical applications of cold atmospheric plasma: State of the science," *Journal of Wound Care*, vol. 27, no. Suppl. 6, pp. S4–S10, 2018.

[12] M. Laroussi, "Plasma medicine: A brief introduction," *Plasma*, vol. 1, no. 1, pp. 47–60, 2018.

[13] Y. Lee, Y. Y. Lee, Y. S. Kim, K. Balaraju, Y. S. Mok, S. J. Yoo, and Y. Jeon, "Enhancement of seed germination and microbial disinfection on ginseng by cold plasma treatment," *Journal of Ginseng Research*, vol. 45, pp. 519–526, 7 2021.

[14] Q. Wang and D. Salvi, "Evaluation of plasma-activated water (paw) as a novel disinfectant: Effectiveness on escherichia coli and listeria innocua, physicochemical properties, and storage stability," *LWT*, vol. 149, p. 111847, 9 2021.

[15] "Polymethylmethacrylate (pmma/acrylic) material properties," 2023. Accessed: 2025-06-16.

[16] "Alumina (aluminum oxide, al□o□) material properties," 2023. Accessed: 2025-06-16.

[17] "Fused quartz/silica (sio□) material properties," 2023. Accessed: 2025-06-16.

[18] “Macor® machinable glass ceramic properties,” 2023. Accessed: 2025-06-16.

[19] “Borosilicate glass material properties,” 2023. Accessed: 2025-06-16.

[20] DuPont, *Teflon® PTFE/PFA Handbook*, 2021. Accessed: 2025-06-16.

[21] BioPak, “What is PLA?,” 2023. Online; accessed 23 May 2025.

[22] D. Parka, M. Jeske, A. Lukanowski, A. Baturo-Ciesniewska, P. Prus, M. Maitah, K. Maitah, K. Malec, D. Rymarz, J. de Dieu Muhire, and K. Szwarc, “Can cold plasma be used for boosting plant growth and plant protection in sustainable plant production?,” *Agronomy*, vol. 12, no. 4, p. 841, 2022.

[23] F. Ciccarese, N. Sasanelli, A. Ciccarese, T. Ziadi, A. Ambrico, and L. Mancini, “Seed disinfestation by ozone treatments,” *Unpublished/ResearchGate*, 2007. Accessed: [Insert Date].

[24] U. Kogelschatz, “Dielectric-barrier discharges: Their History, Discharge Physics, and Industrial Applications,” *Plasma Chemistry and Plasma Processing*, vol. 23, pp. 1–46, 3 2003.

[25] I. Biganzoli, R. Barni, A. Gurioli, R. Pertile, and C. Riccardi, “Experimental investigation of Lissajous figure shapes in planar and surface dielectric barrier discharges,” *Journal of Physics: Conference Series*, vol. 550, p. 012039, 11 2014.

[26] R. Pandiselvam, V. P. Mayookha, A. Kothakota, L. Sharmila, S. V. Ramesh, C. P. Bharathi, K. Gomathy, and V. Srikanth, “Impact of Ozone Treatment on Seed Germination–A Systematic Review,” *Ozone: Science and Engineering*, vol. 42, pp. 331–346, 7 2020.

[27] DFRobot, *Gravity: I2C Ozone Sensor (0-10ppm) SKU SEN0321 Datasheet*. DFRobot, 2023.

[28] E. Systems, *ESP32-S3 Series Datasheet*, 2025. Accessed: June 4, 2025.

[29] DFRobot, *SEN0321 Datasheet*. Sigma Electronica, 2023. Distributor: Sigma Electronica.

[30] Ozone Solutions, “Ozone levels chart,” 2023. Accessed: [Insert Date].

[31] iSafeGas, “SKY2000 O3 Gas Detector,” 2023. Accessed: 2025-06-16.

[32] Conrad, “Fluke 568 infrared thermometer (50:1, -40°c to +800°c, contact measurement).” Online; accessed [Insert Access Date].

[33] C. Buitink and J. Lohman, “Plasma DBD electrodes for a seed disinfection fluidized bed reactor,” June 2024. Bachelor of Science Thesis.

[34] R. Cimerman and K. Hensel, “Multi-hollow Surface Dielectric Barrier Discharge: Production of Gaseous Species Under Various Air Flow Rates and Relative Humidities,” *Plasma Chemistry and Plasma Processing*, vol. 43, pp. 1411–1433, 11 2023.

[35] Lion Lasers, “Laser engraving & cutting machines,” 2023. Accessed: 2025-6-6.

A

Appendix A

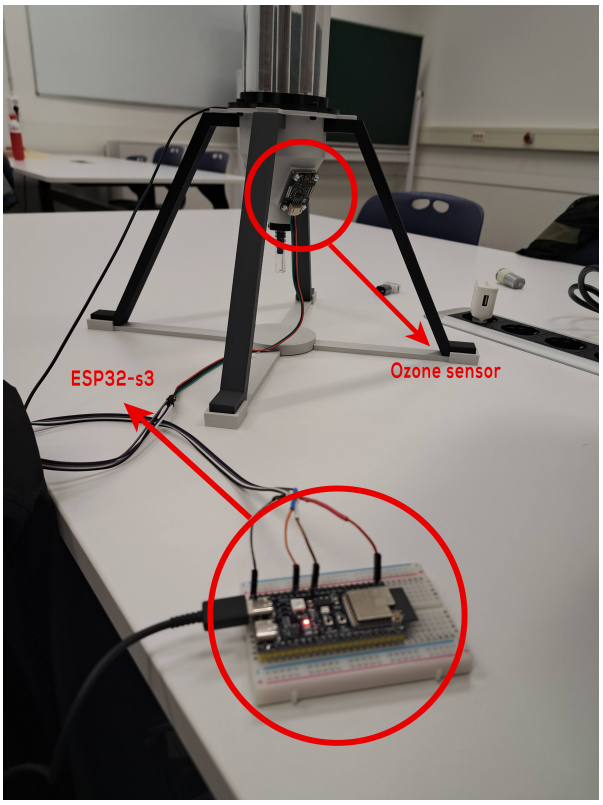

Figure A.1: Calibration setup of the ozone sensor in air

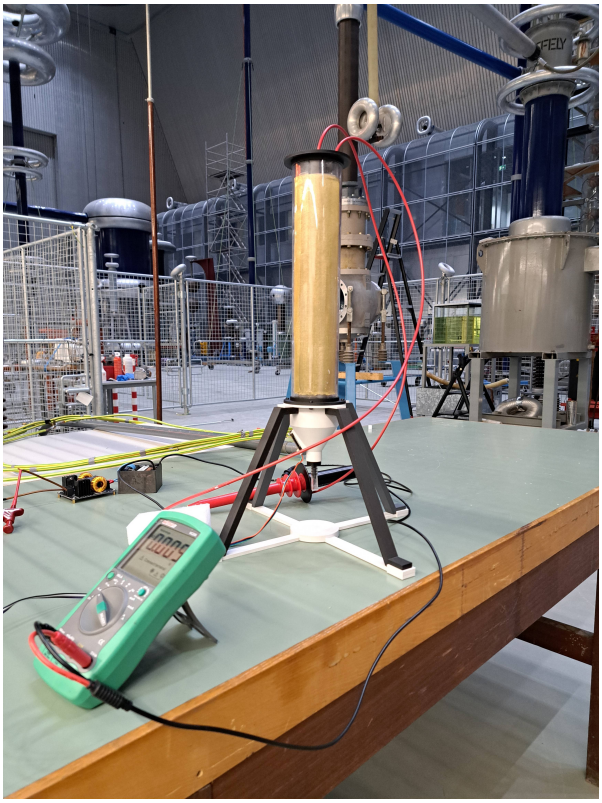

Figure A.2: Test setup of the initial tube setup

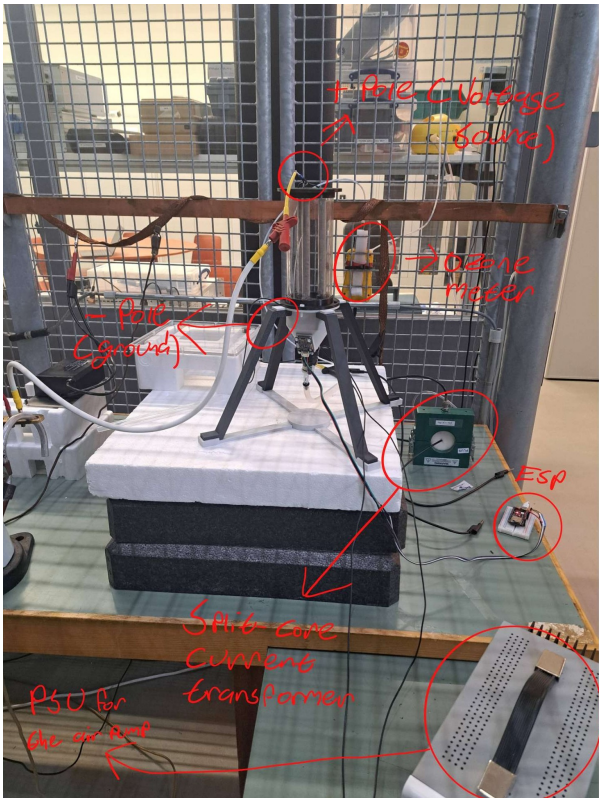

Figure A.3: Test setup of the revised tube setup

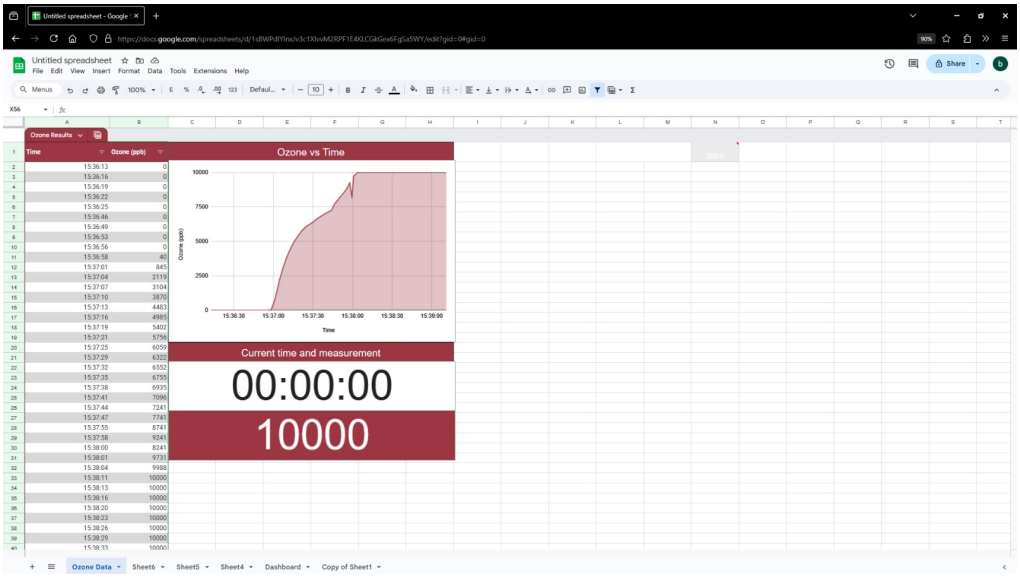

Figure A.4: Ozone sensor measurements dashboard

```python
import pandas as pd
import matplotlib.pyplot as plt
import matplotlib as mpl

mpl.rcParams['agg.path.chunksize'] = 10000  # Fix OverflowError for large plots

# Load the CSV file
df = pd.read_csv('xxx0.csv')  # Update path if necessary

# Shift time so that tmin is t=0
df['Time(s)'] = df['Time(s)'] - df['Time(s)'].min()

# Only plot data where t <= 50 ms
df_plot = df[df['Time(s)']*1000 <= 50]

# Create figure and first axis
fig, ax1 = plt.subplots(figsize=(8, 4))

# Plot CH1 on ax1
ax1.plot(df_plot['Time(s)']*1000, df_plot['CH1(V)'], label='Electrode␣Voltage',
    color='crimson', linewidth=1, alpha=1)
ax1.set_xlabel('Time␣(ms)')
ax1.set_ylabel('␣␣Voltage␣(kV)␣␣', color='black')
ax1.yaxis.set_label_coords(-0.05, 0.5)
ax1.annotate(' ', xy=(-0.0515, 0.34), xycoords='axes␣fraction', color='crimson',
    fontsize=12, ha='right', va='center')

# Create a second y-axis for CH2
ax2 = ax1.twinx()
ax2.plot(df_plot['Time(s)']*1000, df_plot['CH2(V)']*1000, label='Electrode␣Current
    ', color='darkviolet', linewidth=0.5, alpha=1)
ax2.set_ylabel('␣␣Current␣(mA)␣␣', color='black')
ax2.yaxis.set_label_coords(1.05, 0.5)
ax2.annotate(' ', xy=(1.0485, 0.335), xycoords='axes␣fraction', color='darkviolet',
     fontsize=12, ha='left', va='center')

# Find the min/max for both channels
y1_min, y1_max = df['CH1(V)'].min(), df['CH1(V)'].max()
y2_min, y2_max = df['CH2(V)'].min()*1000, df['CH2(V)'].max()*1000

# Find the largest absolute value for symmetric limits
y1_abs_max = max(abs(y1_min), abs(y1_max)) * 1.45
y2_abs_max = max(abs(y2_min), abs(y2_max)) * 1.6

# Set both y-axes to the same symmetric limits around zero
ax1.set_ylim(-y1_abs_max, y1_abs_max)
ax2.set_ylim(-y2_abs_max, y2_abs_max)

# Add grid, title, and legend
ax1.grid(True)
fig.tight_layout()

# Add colored dots to y-axis labels using Unicode and explain in legend
custom_lines = [
    plt.Line2D([0], [0], color='crimson', marker='o', linestyle='None', markersize
        =8, label='Electrode␣Voltage'),
    plt.Line2D([0], [0], color='darkviolet', marker='o', linestyle='None',
        markersize=8, label='Electrode␣Current')
]

```

```
55 fig.legend(handles=custom_lines, loc='upper left', bbox_to_anchor=(0.07, 0.97),
       fontsize=10)
56 plt.savefig('TubeCurrentExample.png', dpi=300, bbox_inches='tight')
57 plt.show()
```

Listing A.1: Plotting voltage and current over the electrode.

```python
import pandas as pd
import numpy as np
import matplotlib.pyplot as plt
import matplotlib.ticker as ticker
from matplotlib.ticker import FuncFormatter, ScalarFormatter

# Load the CSV file
df = pd.read_csv('xxx16.csv')

# Smooth the signals using a rolling average
window_size = 50
VoltageCh1 = df['CH1(V)'].rolling(window=window_size, center=True).mean()
VoltageCh2 = df['CH2(V)'].rolling(window=window_size, center=True).mean()

# Convert to volts and coulombs
Voltage = VoltageCh1 * 1e3       # CH1 in mV → V
Charge = VoltageCh2 * 1e3 * 10e-9  # CH2 in mV → current in µA → integrated to C

# Drop NaNs
Voltage_clean = Voltage.dropna()
Charge_clean = Charge.dropna()

x = Voltage_clean.to_numpy()
y = Charge_clean.to_numpy()

# Convert to kilovolt and microcoulomb for plotting
x_kV = x / 1e3  # V to kV
y_uC = y * 1e6  # C to  C

# Plot
plt.figure(figsize=(8, 6))
plt.plot(x_kV, y_uC, color='royalblue', linewidth=2, alpha=0.9)
plt.fill(x_kV, y_uC, color='royalblue', alpha=0.2, label='Enclosed area')

# Calculate area (energy in joules) remains unchanged
area = 0.5 * np.abs(np.dot(x, np.roll(y, 1)) - np.dot(y, np.roll(x, 1)))
print(f'Enclosed area: {area:.8f} J')

cx = np.mean(x_kV)
cy = np.mean(y_uC)
# Calculate average power if time data is available
if 'Time(s)' in df.columns:
    # Drop NaNs in time column to match processed data
    time_clean = df['Time(s)'].rolling(window=window_size, center=True).mean().
        dropna()
    # Ensure arrays are aligned in length
    min_len = min(len(time_clean), len(x))
    duration = time_clean.iloc[:min_len].iloc[-1] - time_clean.iloc[:min_len].iloc
        [0]
    if duration > 0:
        power = area / duration  # Power in watts
        power_mw = power * 1e3  # Convert to milliwatts
        power_mw_fmt = f"{power_mw:.2f}"  # One decimal place, no scientific
            notation
        print(f'Average power: {power_mw_fmt} mW')
        # Annotate power on plot
        plt.text(cx, cy, f'{power_mw_fmt} mW', fontsize=12, ha='center', va='
            center',
                 bbox=dict(boxstyle='round,pad=0.3', facecolor='white', alpha=0.8)
                     )
```

```
    else:
        print("Duration is zero or negative, cannot compute power.")
else:
    print("No time column found, cannot compute power.")
    # Keep annotation as energy if no time data
    plt.text(cx, cy, f'{area:.2e} J', fontsize=12, ha='center', va='center',
             bbox=dict(boxstyle='round,pad=0.3', facecolor='white', alpha=0.8))

# Labels and style
plt.xlabel('Voltage (kV)', fontsize=12)
plt.ylabel('Charge (C)', fontsize=12)

plt.grid(True, linestyle='--', alpha=0.5)
plt.tight_layout()
plt.tick_params(labelsize=10)
plt.legend()
plt.savefig('TubeLissasous18kVpp.png', dpi=300, bbox_inches='tight')
plt.show()
```

Listing A.2: Plotting Lissajous figure for the electrode and calculating the power.